# Low frequency Compressional modes in degenerate semiconductor plasmas

© Ch. Rozina, N. Maryam¶

Department of Physics, Lahore College for Women University,
Lahore 54000, Pakistan

¶ E-mail: maaryamnaveed@gmail.com

*Received March 12, 2021*
*Revised December 15, 2021*
*Accepted for publication April 24, 2022*

Properties of low frequency compressional electromagnetic wave pulse in a magnetized semiconductor hole-electron plasma, are investigated. The quantum mechanical effects such as Fermi pressure, quantum tunneling and exchange-correlation potential of inertialess electrons, inertial holes and stationary charged ion particulates are considered in the presence of the magnetic field. A new type of dispersion relation is derived for low-frequency compressional waves by employing quantum magneto-hydrodynamic model and Maxwell equations; the dispersion relation is then analyzed for parallel, perpendicular and oblique propagation of compressional electromagnetic wave pulse to the external magnetic field direction. We have analyzed the obtained dispersion relations numerically, for different semiconductor plasma such as GaAs, GaSb and, GaN, the graphs shows that the frequency of compressional electromagnetic wave pulse decreases with increase of electron-hole density concentration, whereas the frequency increases with the increase of angle of propagation compressional electromagnetic wave pulse. Our results are applicable to understanding the dynamics of semiconductor plasma to produce high power, high band-width devices in contrast to the existing gas plasma devices.

**Keywords:** degenerate semiconductor plasma, quantum mechanical effects, compression electromagnetic wave, gas plasma device.

DOI: 10.21883/SC.2022.06.53532.9621a

## 1. Introduction

Quantum plasma is a rapidly growing research area due to its wide range of potential applications such as semiconductor devices [1], quantum computers quantum dots, quantum wires, [2] quantum wells, carbon nano-tubes and diodes [3], ultra-cold [4], metallic and semiconductor nano-structures such as metallic nanoparticles, metal clusters, thin metal films, spintronics [5], electron-hole plasmas [6] and laser-produced plasma experiments, [7] etc. In a system, a gas with all the filled lowest energy quantum states is known as degenerate and the corresponding pressure is called Fermi pressure [8,9], which is a function density concentration of fermions. Such degenerate quantum plasma [10–13] may significantly alter the dispersive properties of linear/nonlinear waves and associated instabilities by taking into account new quantum forces and pressure laws.

One of the important examples of quantum plasma is semiconductor plasma [14–16]. The electron-hole plasma is generated as a result of the interaction between laser pulses and matter. If a semiconductor is excited by a short laser pulse, electrons absorb the photon energy and transit from the valence band to the conduction band, via single or multi photon absorption, depending on the photon energy and band gap energy. This inter band transition of the electrons creates holes in the valence band and this state may satisfy the semiconductor plasma conditions. It has also been observed that in recent semiconductor structures [13], the characteristic scale lengths of impurity variations are comparable to the characteristic electron hole de-Broglie thermal wavelengths. Thus for semiconductor quantum devices [13] working at nano scales, it is quite important to understand and investigate the quantum mechanical effects on the dynamics of the electronhole charge carriers [17]. In this scenario, the dispersive effects of semiconductor plasma are generally due to charge separation between electrons and holes, hence the quantum mechanical effects such as hole-electron Fermi pressure [18], the Bohm tunneling effect of electrons and holes [19] and exchange-correlation force [20] become quite relevant for such plasma. The latter arise due to the Pauli exclusion principle and because of anti-symmetric wave functions [21] associated with different types of exchange interactions between fermions having half spin, opposite spin and fermions of same spin. The exchange potential between degenerate electrons and holes arises due to the parallel spins (having repulsion due to coulomb forces), whereas the correlation potential appear due to correlation between electrons and holes having anti-parallel spins and they are more likely to occupy their nearby locations to reduce the mutual Coulomb repulsion. Therefore, the inclusion of the exchange-correlation (XC) effects in the quantum hydrodynamic (QHD) model plays an important role in the dynamics and total energy of the semiconductor quantum plasma system [22].

Some authors [23,24] have recently investigated the amplitude modulation of the electrostatic waves in electron-hole plasma taking into consideration the effects of the exchange correlation and the Bohm potentials. The

growth rate of modulational instability of a compressional electromagnetic wave in a strongly magnetized electron-positron pair plasma is studied in [25]. The linear and nonlinear propagation of the compressional Alfven wave, having frequency less than the electron-gyro frequency, in collisional electron-hole semiconductors was issued in [24]. Dispersive properties of low-frequency compressional electromagnetic waves are investigated in [26] by using quantum magnetohydrodynamic model and Maxwell equations in cold quantum dusty magnetoplasmas.

In the present manuscript, we shall follow the model presented in [26] to investigate the impact of quantum effects appearing through Fermi pressure, Bohm potential and and electron-hole exchange correlation potential on the dispersive properties of compressional electromagnetic wave pulse (CEMWP) in a magnetized semiconductor quantum plasma. For our purposes, we shall use the QHD model along with Maxwell equations, to derive the dispersion relation for the compressional Alfven waves in magnetized, degenerate electron-hole semiconductor plasma. We shall consider the parallel, perpendicular, and the oblique propagation of CEMWP to investigate the impact of quantum effects appearing through electron-hole Fermi pressure, Bohm Potential and electron-hole exchange correlation potentials on the wave frequencies and the associated wave phase speeds and shall show that the quantum effects may enhance the frequency of CEMWP in semiconductor plasma. The paper is organized in the following fashion: In Sec. II, we develop a new dispersion relation for the compressional Alfven waves in semiconductor quantum magnetoplasmas, by employing the QHD model and Maxwell equations, three particular cases are analyzed to investigate the quantum effects. Section III contains numerical analysis of different semiconductors such as GaAs, GaSb and GaN and discussion on the obtained results is elaborated. A brief summary of the findings is presented in Sec. VII.

## 2. Governing equation

In our present study, we investigate the linear theory of the compressional Alfven wave, whose frequency is lower than the electron-cyclotron frequency, in electron-hole semiconductors taking into account the degenerate hole-electron Fermi pressure, exchange-correlation potential and Bohm potential. Here the interaction between the electrons and the holes is governed by the electrostatic (Hartree) potential and exchange correlation. Moreover, we consider that the Fermi-temperature of electrons or holes is much larger than that of ions, so the quantum recoil force associated with the Bohm potential due to the electrons/holes tunneling through a potential barrier is effective. In our study, we treat electrons and holes as mobile quantum species and according to band theory, we consider ions as immobile species at low temperature. We suppose the compressional Alfven wave is propagating along $x-z$ axis, $\mathbf{k}=(0, k_y, k_z)$, and the external magnetic field is applied along $z-$axis, $\mathbf{B}_0=(0, 0, B_0)$. The quasi-neutrality condition at equilibrium is $n_{e0}=n_{h0}+n_{i0}$ where $n_{s0}$ is the equilibrium number density of species $s$ here the subscripts $e, h, i$ denote electron, hole and ion respectively. The microscopic state of quantum ion plasma is governed by the following linearized set of quantum hydrodynamic and Maxwell equations. The linearized equations of continuity for electrons and holes are respectively

$$\frac{\partial n_{h1}}{\partial t}+n_{h0}(\nabla.\mathbf{U}_{h1})=0, \tag{1}$$

$$\frac{\partial n_{e1}}{\partial t}+n_{e0}(\nabla.\mathbf{U}_{e1})=0. \tag{2}$$

The linearized equations of motion for inertia-less electrons and inertial holes are respectively

$$0=-e\left[\mathbf{E}_1+\frac{\mathbf{U}_{e1}\times\mathbf{B}_0}{c}\right]+\frac{\hbar^2}{4m_e^* n_{e0}}\nabla\nabla^2 n_{e1} - v_{XCe}\nabla\frac{n_{e1}}{n_{e0}}-\frac{2}{3}K_B T_{Fe}\nabla\frac{n_{e1}}{n_{e0}} \tag{3}$$

$$m_h^*\frac{\partial\mathbf{U}_{h1}}{\partial t}=e\left[\mathbf{E}_1+\frac{\mathbf{U}_{h1}\times\mathbf{B}_0}{c}\right]+\frac{\hbar^2}{4m_h^* n_{h0}}\nabla\nabla^2 n_{h1} - v_{XCh}\nabla\frac{n_{h1}}{n_{h0}}-\frac{2}{3}K_B T_{Fh}\nabla\frac{n_{h1}}{n_{h0}} \tag{4}$$

The first and second terms inside the square bracket on r.h.s. of Eqs (3) and (4) is the well known electromagnetic force (or Lorentz force), while the third term represents quantum corrections due to quantum correlation of density fluctuations (also called the quantum Madelung effect which describes the diffraction pattern of plasma species [27]). The fourth terms on r.h.s of Eqs (3) and (4) are the electron exchange-correlation potential, which plays a signi.cant role in the dynamical properties of waves in dense quantum plasmas [28,29], $T_{Fh}$ and $T_{Fe}$ are the Fermi temperatures for holes and electrons respectively defined as

$$\mathbf{T}_{Fe,h}=\frac{\hbar^2 n_{e,h}^{2/3}(3\pi^2)^{2/3}}{2m_{e,h}^* K_B},$$

with $K_B$ as the Boltzmann constant, $m_e^*$ and $m_h^*$ are the effective mass of electrons and holes respectively and $\hbar$ is the Planck constant divided by $2\pi$. The exchange correlation (XC) potential for the electrons and holes is represented as

$$v_{XCe,h}=\frac{0.985e^2}{\epsilon}\left\{1+\frac{0.034}{a_B^* n_{e,h}^{1/3}}\ln\left(1+18.37a_B^* n_{e,h}^{1/3}\right)\right\}n_{e,h}^{1/3}$$

where $a_{Be}^*=\epsilon\hbar^2/m_e e^2$ is the effective Bohr atomic radius and $\epsilon=4\pi\varepsilon_0$ is the relative dielectric constant of the material. Note that the XC potential [13] as function of electron density in Eqs (3), (4) is simply expressed in terms

of electron exchange correlation (XC) speed ($V_{XC}$) through the relation

$$\frac{v_{XCe,h}}{n_{e0,ho}m_{e,h}}\nabla n_{e1,h1} = \frac{V^2_{XCe,h}}{n_{e0,ho}}\nabla n_{e1,h1}$$

where

$$V_{XCe,h} = \left\{\frac{0.985e^2 n^{1/3}_{e0,ho}}{3m_{e,h}\epsilon} + \frac{0.03349e^2 \times 18.37 n^{1/3}_{e0,ho}}{3m_{e,h}\epsilon\left(1+18.37a^*_B n^{1/3}_{e0,ho}\right)}\right\}^{1/2}.$$

The electron-hole XC speed $V_{XCe,h}$, speed significantly alters the dynamical properties of waves and instabilities of degenerate plasma. The last term on r.h.s. of Eqs (3) and (4) indicates the Fermi pressure. The linearized Maxwell equation is

$$\nabla \times \mathbf{E}_1 = -\frac{1}{c}\frac{\partial \mathbf{B}_1}{\partial t} \tag{5}$$

and

$$\nabla \times \mathbf{B}_1 = \frac{4\pi e}{c}\left(n_{h0}\mathbf{U}_{h1} - n_{e0}\mathbf{U}_{e1}\right) \tag{6}$$

where $U_{e1}$ and $U_{h1}$ are the hydrodynamic velocities of the electrons and holes, $e$ is the electronic charge, $c$ is the speed of light, and $E_1$ is the electric field vector. We have also neglected the displacement current in Eq. (6) because we are focusing the waves whose phase speed is much smaller than the speed of light. Calculating $U_{e1}$ from Eq. (6) and substituting into Eq. (3), we obtain

$$\mathbf{E}_1 = -\frac{1}{c}\left(\mathbf{U}_{h1}\times\mathbf{B}_0\right)\frac{n_{h0}}{n_{e0}} + \frac{1}{4\pi e n_{e0}}\left(\nabla\times\mathbf{B}_1\right)\times\mathbf{B}_0 + \frac{\hbar^2}{4m^*_e n_{e0.}e}\nabla\nabla^2 n_{e1} - \frac{m^*_e}{e}V^2_{xce}\nabla\frac{n_{e1}}{n_{e0}} - \frac{2}{3e}K_B T_{Fe}\nabla\frac{n_{e1}}{n_{e0}} \tag{7}$$

Using Eq. (7) and the charge-neutrality condition

$$\frac{n_{i0}}{n_{e0}} = 1 - \frac{n_{h0}}{n_{e0}},$$

Eq. (4) can be simplified as

$$\frac{\partial \mathbf{U}_{h1}}{\partial t} = \left\{-\Omega_R(\mathbf{U}_{h1}\times\hat{z}) - \frac{\nabla(\mathbf{B}_0.\mathbf{B}_1)}{4\pi m^*_h n_{e0}} + \frac{(\mathbf{B}_0.\nabla)\mathbf{B}_1}{4\pi m^*_h n_{e0}} + \frac{\hbar^2}{4m^*_e n_{e0}m^*_h}\nabla\nabla^2 n_{e1} - \mu V^2_{xce}\nabla\frac{n_{e1}}{n_{e0}} - V^2_{xch}\nabla\frac{n_{h1}}{n_{h0}} - \frac{2}{3m^*_h}K_B T_{Fe}\nabla\frac{n_{e1}}{n_{e0}} - \frac{2}{3m^*_h}K_B T_{Fh}\nabla\frac{n_{h1}}{n_{h0}}\right\}$$

Let us rewrite above equation as

$$\frac{\partial \mathbf{U}_{h1}}{\partial t} = \left\{-\Omega_R(\mathbf{U}_{h1}\times\hat{z}) + \frac{1}{4\pi m^*_h n_{e0}}\left\{\left(\nabla\times\mathbf{B}_1\right)\times\mathbf{B}_0\right\} + \frac{\hbar^2}{4m^*_e n_{e0}m^*_h}\nabla\nabla^2 n_{e1} - \mu V^2_{xce}\nabla\frac{n_{e1}}{n_{e0}} - V^2_{xch}\nabla\frac{n_{h1}}{n_{h0}} - \frac{2}{3}V^2_s\nabla\frac{n_{e1}}{n_{e0}}\right\}. \tag{8}$$

Where $\hat{z}$ is the unit vector along $z$-axis,

$$\mu = \frac{m^*_e}{m^*_h}, \quad \Omega_R = \left(\frac{n_{i0}}{n_{e0}}\right)\omega_{ci}$$

is the Rao cutoff frequency,

$$\omega_{ci} = \frac{eB_0}{m^*_h c}$$

is the hole gyro frequency,

$$V^2_{se} = \frac{2K_B T_{Fe}}{3m^*_h}, \quad V^2_{fh} = \frac{K_B T_{Fh}}{m^*_h} \quad \text{and} \quad V^2_s = V^2_{se} + V^2_{fh}.$$

Now substituting Eq. (7) in Eq. (5) and using identity $\nabla\times(\nabla f) = 0$, we are left with

$$\frac{\partial \mathbf{B}_1}{\partial t} = \frac{n_{h0}}{n_{e0}}\left[-\mathbf{B}_0(\nabla.\mathbf{U}_{h1}) + (\mathbf{B}_0.\nabla)\mathbf{U}_{h1}\right] \tag{9}$$

One may have from Eq. (8)

$$\frac{\partial \mathbf{U}_{h\perp}}{\partial t} = -\Omega_R(\mathbf{U}_{h1}\times\hat{z}) - \frac{B_0\nabla_\perp B_1}{4\pi m^*_h n_{e0}} + \frac{\hbar^2}{4m^*_e n_{e0}m^*_h}\nabla\nabla^2 n_{e1} - V^2_{xch}\nabla\frac{n_{h1}}{n_{h0}} - \left(\mu V^2_{xce} + \frac{2}{3}V^2_s\right)\nabla\frac{n_{e1}}{n_{e0}}. \tag{10}$$

Taking $\hat{z}$-component of Eq. (10)

$$\frac{\partial \mathbf{U}_{hz}}{\partial t} = \frac{\hbar^2}{4m^*_e n_{e0}m^*_h}\frac{\partial}{\partial Z}\nabla^2 n_{e1} - \frac{2}{3}V^2_s\frac{\partial}{\partial Z}\frac{n_{e1}}{n_{e0}} - \mu V^2_{xce}\frac{\partial}{\partial Z}\frac{n_{e1}}{n_{e0}} - V^2_{xch}\frac{\partial}{\partial Z}\frac{n_{h1}}{n_{h0}} \tag{11}$$

According to the chosen geometry Eq. (9) left with as

$$\frac{\partial \mathbf{B}_1}{\partial t} = -\frac{n_{h0}}{n_{e0}}\mathbf{B}_0(\nabla_\perp.\mathbf{U}_{h1}) \tag{12}$$

Now taking the time derivative on both sides of Eq. (10), we have

$$\frac{\partial^2 \mathbf{U}_{h\perp}}{\partial t^2} = \left\{-\Omega_R\left(\frac{\partial \mathbf{U}_{h1}}{\partial - t}\times\hat{z}\right) + \frac{\partial}{\partial t}\left(\frac{-B_0\nabla_\perp B_1}{4\pi m^*_h n_{e0}} + \frac{\hbar^2}{4m^*_e n_{e0}m^*_h}\nabla\nabla^2 n_{e1}\right) - \frac{\partial}{\partial t}V^2_{xch}\nabla_\perp\frac{n_{h1}}{n_{h0}} - \frac{\partial}{\partial t}\left(\frac{2}{3}V^2_s + \mu V^2_{xce}\right)\nabla_\perp\frac{n_{e1}}{n_{e0}}\right\}. \tag{13}$$

Eliminating $\frac{\partial \mathbf{U}_{h1}}{\partial t}$ from Eqs. (13) and (10) and then taking the divergence of the holes fluid velocity $U_{h\perp}$, we eventually

obtain

$$\left(\frac{\partial^2}{\partial t^2}+\Omega_R^2\right)\nabla_\perp.\mathbf{U}_{h1}=\left\{-\frac{B_0}{4\pi m_h^* n_{e0}}\left[\left(\nabla_\perp^2\frac{\partial}{\partial t}+\Omega_R\nabla_\perp.(\hat{z}\times\nabla_\perp)\right)\times\left(\mathbf{B}_1-\frac{\pi\hbar^2\nabla^2 n_{e1}}{m_e^* B_0}\right)\right]+\Omega_R\left[\left(\frac{2}{3}V_s^2+\mu V_{xce}^2\right)\nabla_\perp.(\nabla_\perp\times\hat{z})\frac{n_{e1}}{n_{e0}}+V_{xch}^2\nabla_\perp.(\nabla_\perp\times\hat{z})\frac{n_{h1}}{n_{h0}}\right]-\frac{\partial}{\partial t}\left[\left(\frac{2}{3}V_s^2+\mu V_{xce}^2\right)\nabla_\perp^2\frac{n_{e1}}{n_{e0}}+V_{xch}^2\nabla_\perp^2\frac{n_{h1}}{n_{h0}}\right]\right\}. \quad (14)$$

A more simplified form of Eq. (14) is obtained by using Eq. (12) and taking into account the identity $\nabla_\perp.(\hat{z}\times\nabla_\perp\phi)=0$

$$\left(\frac{\partial^2}{\partial t^2}+\Omega_R^2-\nabla_\perp^2V_A^2\right)B_1=\left(-\alpha_q\nabla_\perp^2B_0\nabla^2+B_0\frac{n_{h0}}{n_{e0}}V_s^2\nabla_\perp^2+V_{xch}^2\nabla_\perp^2B_0+\mu V_{xce}^2\nabla_\perp^2\frac{n_{h0}}{n_{e0}}B_0\right)\frac{n_{e1}}{n_{e0}}. \quad (15)$$

Here

$$V_A=\frac{n_{h0}}{n_{e0}}\frac{B_0}{\sqrt{4\pi m_h^* n_{e0}}}$$

is the Alfven speed, and

$$\alpha_q=\left(\frac{n_{h0}}{n_{e0}}\right)\frac{\hbar^2}{4m_h^*m_e^*}$$

is the Alfven speed, and

$$\alpha_q=\left(\frac{n_{h0}}{n_{e0}}\right)\frac{\hbar^2}{4m_h^*m_e^*}$$

is a quantum parameter. Using quasi-neutrality condition, $n_{e1}\backsimeq n_{h1}$ let us rewrite Eq. (1) as

$$\frac{\partial n_{e1}}{\partial t}+n_{h0}(\nabla_\perp.U_{h1})+n_{h0}\frac{\partial}{\partial z}U_{hz}=0. \quad (16)$$

Now multiplying Eq. (16) by $(\frac{\partial^2}{\partial t^2}+\Omega_R^2)$ and inserting Eqs (11) and (14) into theresultant equation, we may obtain

$$\left[\left(\frac{\partial^2}{\partial t^2}+\Omega_R^2\right)\left(\frac{\partial^2}{\partial t^2}+\alpha_q\frac{\partial^2}{\partial Z^2}\nabla^2-\left(V_s^2+\mu V_{xce}^2\right)\frac{\partial^2}{\partial Z^2}\frac{n_{h0}}{n_{e0}}-V_{xch}^2\frac{\partial^2}{\partial Z^2}\right)+\alpha_q\nabla_\perp^2\nabla^2\frac{\partial^2}{\partial t^2}-\frac{\partial^2}{\partial t^2}V_{xch}^2\nabla_\perp^2-\frac{\partial^2}{\partial t^2}\left(V_s^2+\mu V_{xce}^2\right)\nabla_\perp^2\frac{n_{h0}}{n_{e0}}\right]\times n_{e1}=\left(\frac{n_{h0}}{n_{e0}}.\frac{B_0\nabla_\perp^2}{4\pi m_h^*}\frac{\partial^2B_1}{\partial t^2}\right). \quad (17)$$

Substituting the value of perturbed magnetic field $B_1$ from Eq. (15) into Eq. (17) and applying Fourier transformation, we shall obtain the general dispersion equation

$$0=\left\{\left[\begin{array}{l}(\omega^2-\Omega_R^2)\left(\omega^2-\alpha_qk_z^2k^2-V_{xch}^2k_z^2\right.\\ \left.-\left(V_s^2+\mu V_{xce}^2\right)k_z^2\frac{n_{h0}}{n_{e0}}\right)-\alpha_q\omega^2k_\perp^2k^2\\ -\omega^2k_\perp^2V_{xch}^2-\omega^2\left(V_s^2+\mu V_{xce}^2\right)k_\perp^2\frac{n_{h0}}{n_{e0}}\end{array}\right]\times(\omega^2-\Omega_R^2-k_\perp^2V_A^2)-V_A^2k_\perp^4\omega^2\alpha_qk^2-V_A^2k_\perp^4\omega^2\frac{n_{h0}}{n_{e0}}V_s^2-V_A^2k_\perp^4\omega^2V_{xch}^2-V_A^2\mu V_{xce}^2k_\perp^4\omega^2\frac{n_{h0}}{n_{e0}}\right\} \quad (18)$$

Eq. (18) represents the dispersion relation of the CEMWP in magnetized, quantum electron-hole semiconductor plasma. Initially for an electron-hole plasma, we assume $\Omega_R\to 0$,

$$V_A=\frac{n_{h0}}{n_{e0}}\frac{B_0}{\sqrt{4\pi m_h^* n_{e0}}}=V_a,$$

and

$$\alpha_q=\left(\frac{n_{h0}}{n_{e0}}\right)\frac{\hbar^2}{4m_h^*m_e^*}=\alpha,$$

to re-write Eq. (18)

$$\omega^4-B\omega^2+C=0 \quad (19)$$

which admits the solution

$$\omega^2=\frac{1}{2}\left[B\pm\sqrt{B^2-4C}\right] \quad (20)$$

where

$$B=\alpha k^4+\frac{n_{h0}}{n_{e0}}V_s^2k^2+k^2V_{xch}^2+\mu V_{xce}^2k^2\frac{n_{h0}}{n_{e0}}+k_\perp^2V_a^2$$

and

$$C=k_\perp^2V_a^2\alpha k_z^2k^2+k_z^2k_\perp^2V_a^2\frac{n_{h0}}{n_{e0}}V_s^2+k_\perp^2V_a^2V_{xch}^2k_z^2+\mu V_{xce}^2k_\perp^2V_a^2k_z^2\frac{n_{h0}}{n_{e0}}$$

We shall analyze the dispersion relation shown in Eq. (18) for three special cases, i.e., for parallel, perpendicular, and oblique propagation. For this purpose, we shall symbolize $k_z(=k\cos\theta)$ as parallel and $k_\perp(=k\sin\theta)$ perpendicular wave vectors, then let us rewrite Eq. (18) as

$$\omega^6-A\omega^4+B\omega^2-C=0 \quad (21)$$

where

$$A=2\Omega_R^2+k^2\left[\alpha_qk^2+\left(V_s^2+\mu V_{xce}^2\right)\frac{n_{h0}}{n_{e0}}+V_{xch}^2+V_A^2\sin^2\theta\right],$$

$$B = \left\{\Omega_R^2\left[\Omega_R^2 + 2\left(\alpha_q k^2 + V_{xch}^2\right)k^2\cos^2\theta + \left(\alpha_q k^2 + V_{xch}^2 + V_A^2\right)k^2\sin^2\theta\right] + k^4V_A^2\left(k^2\alpha_q + V_{xch}^2\right) \times \sin^2\theta\cos^2\theta + \left[2\Omega_R^2\left(V_s^2 + \mu V_{xce}^2\right)k^2\cos^2\theta + \Omega_R^2\left(V_s^2 + \mu V_{xce}^2\right)k^2\sin^2\theta + k^4V_A^2\left(V_s^2 + \mu V_{xce}^2\right) \times \sin^2\theta\cos^2\theta\right]\frac{n_{h0}}{n_{e0}}\right\}$$

and

$$C = \left\{\Omega_R^2\left[\Omega_R^2k^2\left(k^2\alpha_q + V_{xch}^2\right) + k^4V_A^2\left(k^2\alpha_q + V_{xch}^2\right)\sin^2\theta\right] \times \cos^2\theta + \Omega_R^2\left[\Omega_R^2\left(V_s^2 + \mu V_{xce}^2\Omega_R^2\right)k^2 + V_A^2\left(V_s^2 + \mu V_{xce}^2\right)k^4\sin^2\theta\right]\cos^2\theta\frac{n_{h0}}{n_{e0}}\right\}.$$

Next, we shall investigate dispersion Eq. (21) for some particular cases.

### A. Case I (parallel propagation)

For parallel propagation, Eq. (21) reduces to

$$(\omega^2 - \Omega_R^2)^2(\omega^2 - \alpha_q k^4 - k^2V_s^2 - k^2V_{xch}^2 - \mu V_{xce}^2k^2) = 0. \tag{22}$$

It is quite important to note here that for $\alpha_q = 0$, it was shown in [26] that the propagation vector in Eq. (22) vanishes, and only the cutoff exists but in case of semiconductor it is quite evident from Eq. (22) that situation is quite different the four possible solutions of above equation are

$$\omega = \Omega_R,\ -\Omega_R;$$
$$\omega = k\sqrt{\left(\alpha_q k^2 + V_s^2\frac{n_{h0}}{n_{e0}} + V_{xch}^2 + \mu V_{xce}^2\frac{n_{h0}}{n_{e0}}\right)},$$
$$-k\sqrt{\left(\alpha_q k^2 + V_s^2\frac{n_{h0}}{n_{e0}} + V_{xch}^2 + \mu V_{xce}^2\frac{n_{h0}}{n_{e0}}\right)} \tag{23}$$

For graphical representation, Eq. (23) is normalized by the scaled parameters such as $K = k\lambda_{fe}$ where $\lambda_{f_e} = \frac{V_{fe}}{\omega_{pe}}$ and $\gamma = \frac{\omega}{\omega_{pe}}$ then the normalized expression of Eq. (23) will be

$$\gamma = \sqrt{P^2K^4 + K^2V_s^{2*} + K^2V_{xch}^{2*} + \mu K^2V_{xce}^{2*}} \tag{24}$$

where

$$P^2 = \frac{\hbar^2\omega_{pe}^2}{4V_{fe}^4m_e^*m_h^*},\ V_s^{2*} = \frac{V_s^2}{V_{fe}^2},\ V_{xch}^{2*} = \frac{V_{xch}^2}{V_{fe}^2},\ V_{xce}^{2*} = \frac{V_{xce}^2}{V_{fe}^2}.$$

### B. Case II (perpendicular propagation)

For the perpendicular propagation, we may obtain from Eq. (21) the dispersion relation for the compressional modes in quantum electron-hole plasma

$$\omega^4 - \omega^2 + C = 0. \tag{25}$$

The possible solution of above equation

$$\omega^2 = \frac{1}{2}\left[B \pm \sqrt{B^2 - 4C}\right] \tag{26}$$

where

$$B = 2\Omega_R^2 + \alpha_q k^4 + k^2V_A^2 + k^2\frac{n_{h0}}{n_{e0}}V_s^2 + V_{xch}^2k^2 + \mu V_{xce}^2k^2\frac{n_{h0}}{n_{e0}}$$

and

$$C = \Omega_R^4 + \alpha_q\Omega_R^2k^4 + k^2V_A^2\Omega_R^2 + \Omega_R^2k^2\frac{n_{h0}}{n_{e0}}V_s^2 + \Omega_R^2V_{xch}^2k^2 + \Omega_R^2\mu V_{xce}^2k^2\frac{n_{h0}}{n_{e0}}.$$

Here if $\Omega_R = 0$ than above equation reduces to

$$\omega = k\sqrt{\alpha k^2 + V_a^2 + V_s^2 + V_{xch}^2 + \mu V_{xce}^2}. \tag{27}$$

Similarly, we can normalize the angular frequency $\omega$ of Alfven waves given in Eq. (27) by using the normalized parameters mentioned above to obtain

$$\gamma = \sqrt{P^2K^4 + K^2V_a^{2*} + K^2V_s^{2*} + K^2V_{xch}^{2*} + \mu K^2V_{xce}^{2*}}. \tag{28}$$

### C. Case III (oblique propagation)

For oblique propagation, we shall ignore ions, i.e., $\Omega \to 0$, to rewrite Eq. (21) as to obtain

$$\omega^4 - B\omega^2 + C = 0$$

The possible solution of above equation

$$\omega^2 = \frac{1}{2}\left[B \pm \sqrt{B^2 - 4C}\right] \tag{29}$$

where

$$B = \alpha_q k^4 + k^2\sin^2\theta V_A^2 + k^2V_s^2 + V_{xch}^2k^2 + \mu V_{xce}^2k^2,$$

and

$$C = \alpha_q k^6\cos^2\theta\sin^2\theta V_A^2 + k^4\sin^2\theta V_A^2\cos^2\theta V_s^2 + k^4\sin^2\theta V_A^2\cos^2\theta V_{xch}^2 + \sin^2\theta V_A^2k^4\cos^2\theta\mu V_{xce}^2$$

The normalized expression of Eq. (28) will be written as

$$\gamma = \frac{1}{2}K^2\left\{P^2K^2 + V_a^{2*}\sin^2\theta + V_s^{2*} + V_{xch}^{2*} + \mu V_{xce}^{2*} + \sqrt{\begin{array}{l}\left(P^2K^2 + V_a^{2*}\sin^2\theta + V_s^{2*} + V_{xch}^{2*} + \mu V_{xce}^{2*}\right)^2 \\ -4\left(P^2K^2 + V_s^{2*} + V_{xch}^{2*} + \mu V_{xce}^{2*}\right)V_a^{2*}\sin^2\theta\cos^2\theta\end{array}}\right\} \tag{30}$$

## 3. Numerical results and discussion

In this section, we shall numerically study the effects of variations of electron-hole concentration on the propagation of CEMWP. The three semiconductors such as GaAs, GaSb and GaN are chosen for our investigation, having typical parameters for GaAs [13] $n_0 = 4.7 \cdot 10^{16}\,\mathrm{cm}^{-3}$ ($n_0 \approx n_{h0} \approx n_{e0}$), $m_e^* = 0.067 m_e$ g ($m_e$ is the mass of electron), $m_h^* = 0.5 m_e$ g, and $\epsilon = 12.8$, for GaSb $n_0 = 1.6 \cdot 10^{17}\,\mathrm{cm}^{-3}$, $m_e^* = 0.047 m_e$ g, $m_h^* = 0.4 m_e$ g and $\epsilon = 11.3$, and for GaN the parameters are $n_0 = 10^{17} - 10^{20}\,\mathrm{cm}^{-3}$, $m_e^* = 0.13 m_e$ g, $\epsilon = 1.3 m_e$ g and $\epsilon = 11.3$. By using this semiconductors data, we shall plot numerically Eqs (24), (28) and (30) in Figs (1–3) respectively to study the dispersion properties of the compressional modes in semiconductor quantum magnetoplasmas. For parametric analysis, initially to show the impact of quantum effects on the frequency of CEMWP, we take typical parameters for GaAs and normalized propagation vector $K(= k\lambda_{fe}) = 2$ in Eq. (24); to find electron plasma frequency $\omega_{pe} = 1.22 \cdot 10^{13}\,\mathrm{s}^{-1}$, Fermi speed $V_{fe} = 1.11 \cdot 10^7$ cm/s, the exchange correlation potential for the electrons $V_{XCe} = 6.1 \cdot 10^6$ cm/s and for holes $V_{XCh} = 2.5 \cdot 10^6$ cm/s, quantum parameter $\alpha_q \left(= \frac{n_{h0}}{n_{e0}} \frac{\hbar^2}{4 m_h^* m_e^*}\right) = 9.94 (\mathrm{erg\text{-}s})^2 \mathrm{g}^{-2}$ and the associated frequency of the CEMWP $\omega = 1.31\omega_{pe}$. However, by increasing $V_{XCe} = 6.8 \cdot 10^6$ cm/s (via $n_{e0} = 9 \cdot 10^{16}\,\mathrm{cm}^{-3}$) and keeping all the other parameters fixed, we come up with higher value of frequency of CEMWP $\omega = 1.57\omega_{pe}$. Hence, the parametric analysis clearly shows that quantum effects enhance the frequency of CEMWP in semiconductor plasma.

Next, to see how electron-hole density alters the frequency of CEMWP, we take GaAs semiconductor and at $n_0 = 4.7 \cdot 10^{16}\,\mathrm{cm}^{-1}$, the frequency of the CEMWP $\omega = 1.31\omega_{pe}$. However, for GaN with density $n_0 = 1.6 \cdot 10^{17}\,\mathrm{cm}^{-3}$, we trace that the corresponding frequency of the CEMWP gets reduced in magnitude to $\omega = 0.925\omega_{pe}$. This parametric analysis elaborates that as we increase the electron-hole density, the corresponding frequency of CEMWP decreases.

Fig. 1 is plotted for the normalized frequency $\gamma$, of Alfven waves as a function of the parallel component of normalized propagation vector $K$ shown in Eq. (24) for the semiconductors under consideration. Plot clearly depicts that the presence of Fermi pressure, Bohm Potential and exchange-correlation force in the momentum equations for electrons and holes modifies the frequency spectrum of CEMWP in the sense that at low values of electron-hole density, the frequency of CEMWP is large and vice versa. It is also clear from the graph that the frequency of all three semiconductors are almost same in case of small propagation vector, however these frequencies are quite apart at short wavelength scales. Figure 2 shows the variation of the normalized angular frequency, $\gamma$ and the normalized Alfven speed, for the perpendicular propagation

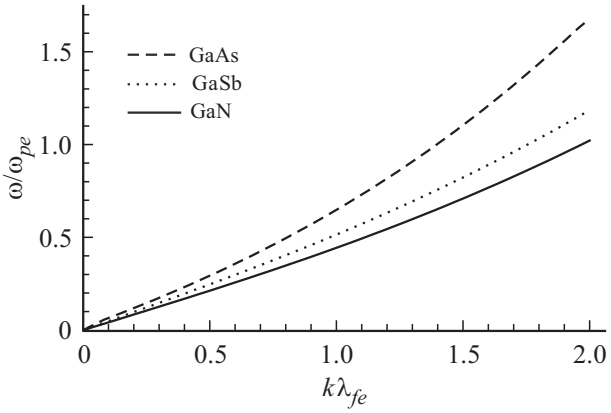


**Figure 1.** The normalized growth rate ($\gamma = \omega/\omega_{pe}$) shown in Eq. (24) is plotted against the parallel component of normalized propagation vector ($K = k\lambda_{fe}$) for different semiconductors [GaAs (dashed curve), GaSb (dotted curve), GaN (solid curve)].

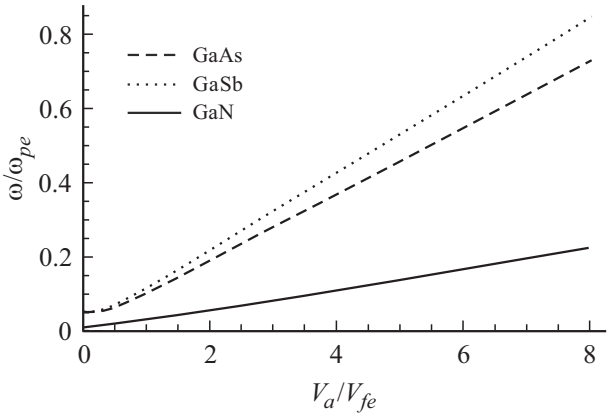


**Figure 2.** The normalized growth rate ($\gamma = \omega/\omega_{pe}$) presented in Eq. (28) is plotted against the normalized Alfven speed ($V_\alpha/V_{fe}$) for different semiconductors [GaSb (dotted curve), GaAs (dashed curve), GaN (solid curve)].

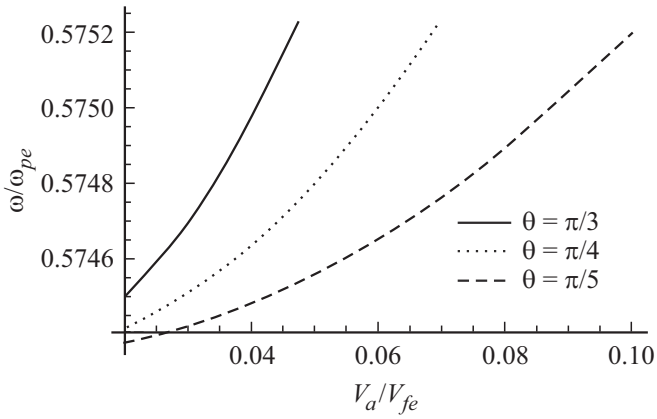


**Figure 3.** The normalized growth rate ($\gamma = \omega/\omega_{pe}$) [as described by Eq. (30)] is plotted against the normalized Alfvén speed ($V_\alpha = V_{fe}$) for different angles of propagation [$\theta = \pi/5$ (dashed curve), $\theta = \pi/4$ (dotted curve), $\theta = \pi/3$ (solid curve)] by keeping the perpendicular component of the propagation vector fixed a $k_\perp = 10^6\,\mathrm{cm}^{-1}$.

of CEMWP as shown in Eq. (28), plot shows that the frequency of CEMWP is low for the GaN having high density, whereas for GaAS (with lowest electron-hole density concentration) it is large enough. Fig. 3 displays the plot between the normalized growth rate ($\gamma = \omega/\omega_{pe}$) and the normalized Alfven speed ($V_\alpha/V_{fe}$) for oblique angles of propagation [$\theta = \pi/5,\ \theta = \pi/4,\ \theta = \pi/3$], for fixed values of number densities with $K = 10^6\,\mathrm{cm}^{-1}$ for GaAs. We observed that the frequency of the compressional Alfven waves increase as we go on increasing the angle of propagation vector of CEMWP. In other words, the frequency of the compressional Alfven waves is altered for different angles of propagations.

## 4. Conclusion

We have studied the linear propagation of CEMW in quantum semiconductor electronhole plasma with the inclusion of degenerate Fermi pressure, Bohm potential, and exchange correlation potential effects of both electrons and holes. We have followed quantum magnetohydrodynamics and Maxwell's equations to develop the dispersion relation for low frequency compressional Alfven waves in semiconductor electron-hole quantum plasma. Our theoretical results are then applied numerically to three kinds of semiconductor plasma: namely, GaAs, GaSb, GaN. The quantum effects are found to be quite important to significantly enhance the phase speed of CEMWP in a semiconductor plasma. The impact of electron hole density variations on linear propagation of CEMWP structures is investigated. The results are useful for understanding the energy transport mechanism in semiconductor electron-hole plasma in the parallel, perpendicular and oblique propagation of CEMWP to the applied magnetic field. Present investigation may also be useful for the understanding of semiconductor plasma in order to produce high power, high band-width devices [30].

## References


[1] P.A. Markowich, C.A. Ringhofer, C. Schmeiser. *Semiconductor Equations* (Springer Verlag, N.Y., 1990).
[2] G.V. Shpatakovskaya. J. Exp. Theor. Phys., **102**, 466 (2006).
[3] L.K. Ang, T.J.T. Kwan, Y.Y. Lau. Phys. Rev. Lett., **91**, 208303 (2003); L.K. Ang. IEEE Trans. Plasma Sci., **32**, 410 (2004); L.K. Ang, W.S. Koh, Y.Y. Lau, T.J.T. Kwan. Phys. Plasmas, **13**, 056701 (2006); L.K. Ang, P. Zhang. Phys. Rev. Lett., **98**, 164802 (2007).
[4] T.C. Killian. Nature (London), **441**, 297 (2006).
[5] S.M. Lindsay. *Introduction to Nanoscience* (Oxford University Press, Oxford, 2010).
[6] Y.D. Jung. Phys. Plasmas, **8**, 3842 (2001); M. Opher, L.O. Silva, D.E. Dauger, V.K. Decyk, J.M. Dawson. Physics Plasmas, **8**, 2454 (2001); S.H. Glenzer, O.L. Landen, P. Neumayer. Phys. Rev. Lett., **98**, 065002 (2007).
[7] G. Barak, H. Steinberg, L.N. Pfeiffer, K.W. West, L. Glazman, F. von Oppen, A. Yacoby. Nature Physics, **6**, 489 (2010).
[8] G.A. Truscott, E.K. Strecker, W.I. McAlexander, G. Partridge, R.G. Hulet. Science, **291**, 2570 (2001).
[9] Ch. Rozina, S. Ali, H.A. Shah, M. Jamil. Physics Plasmas, **25**, 092903 (2018).
[10] M. Marklund, G. Brodin. Phys. Rev. Lett., **98**, 025001 (2007); G.Brodin, M. Marklund, J. Zamanian, A. Ericsson, P.L. Mana. Phys. Rev. Lett., **101**, 245002 (2008).
[11] L. Hedin, B.I. Lundqvist. J. Phys. C, **4**, 2064 (1971); L. Brey, J. Dempsey, N.F. Johnson, B.I. Halperin. Phys. Rev. B, **42**, 1240 (1990).
[12] P. Hohenberg, W. Kohn. Phys. Rev., **136**, B864 (1964).
[13] Sourav Choudhury, Tushar Kanti Das, Malay Kr. Ghorui, Prasanta Chatterjee. Physics Plasmas, **24**, 062103 (2017).
[14] C. Gardner. SIAM J. Appl. Math.,**54**, 409 (1994).
[15] N. Crouseilles, P.-A. Hervieux, G. Manfredi. Phys. Rev. B, **78**, 155412 (2008).
[16] S.A. Maier. *Plasmonics* (Springer, N.Y., 2007); M.F. Tsai, H. Lin, C. Lin, S. Lin, S. Wang, M. Lo, S. Cheng, M. Lee, W. Chang. Phys. Rev. Lett., **101**, 267402 (2008).
[17] F. Areeb, A. Rasheed, M. Jamil, M. Siddique, P. Sumera. Physics Plasmas, **25**, 012111 (2018).
[18] N.L. Tsintsadze, L.N. Tsintsadze, A. Hussain, G. Murtaza. Eur. Phys. J. D, **64**, 447 (2011).
[19] F. Haas, L.G. Garcia, J. Goedert, G. Manfredi. Physics Plasmas, **10**, 3858 (2003).
[20] L. Brey, J. Dempsey, N.F. Johnson, B.I. Halperin. Phys. Rev. B, **42**, 1240 (1990).
[21] M. Trukhanova, P. Andreev. Physics Plasmas, **22**, 022128 (2015).
[22] M.E. Yahia, I.M. Azzouz, W.M. Moslem. Appl. Phys. Lett., **103**, 082105 (2013).
[23] Y. Wang, B. Eliasson. Phys. Rev. B, **89**, 205316 (2014); Y. Wang, X. Leu. Physics Plasmas, **21**, 022107 (2014).
[24] M.R. Amin. Physics Plasmas, **22**, 032303 (2015).
[25] M. R. Amin. Phys. Rev. E, **92**, 033106 (2015).
[26] S. Ali, P.K. Shukla. Physics Plasmas, **13**, 052113 (2006).
[27] G.A. Biberman, N. Sushkin, V. Fabrikant, Dock1. Akad. Nauk USSR, **26**, 185 (1994).
[28] F. Brosens, J. Devreese. Phys. Rev. B, **29**, 543 (1984); S.-H. Mao, J.-K. Xue. Phys. Scr., **84**, 055501 (2011).
[29] H. Cai-Xia, X. Ju-Kui. Chin. Phys. B, **22**, 025202 (2013); Y.-T. Ma, S.-H. Mao, J.-K. Xue. Physics Plasmas, **18**, 102108 (2011).
[30] S.Y. Liao. *Microwave Solid-State Devices* (Prentice Hall, Englewood Cliffs, N.J., 1985) p. 167.